SEISMIC FACIES CHARACTERIZATION BY SCALE ANALYSIS

Felix J. Herrmann

Earth Resources Laboratory
Department of Earth, Atmospheric, and Planetary Sciences
Massachusetts Institute of Technology
Cambridge, MA 02139

ABSTRACT

Over the years, there has been an ongoing struggle to relate well-log and seismic data due to the inherent bandwidth limitation of seismic data, the problem of seismic amplitudes, and the apparent inability to delineate and characterize the transitions that can be linked to and held responsible for major reflection events and their signatures. By shifting focus to a scale invariant sharpness characterization for the reflectors, we develop a method that can capture, categorize, and reconstruct the main features of the reflectors, without being sensitive to the amplitudes. In this approach, sharpness is defined as the fractional degree of differentiability, which refers to the order of the singularity of the transitions. This sharpness determines mainly the signature/waveform of the reflection and can be estimated with the proposed monoscale analysis technique. Contrary to multiscale wavelet analysis the monoscale method is able to find the location and sharpness of the transitions *at* the fixed scale of the seismic wavelet. The method also captures the local orders of magnitude of the amplitude variations by scale exponents. These scale exponents express the local scale-invariance and texture. Consequently, the exponents contain local information on the type of depositional environment to which the reflector pertains. By applying the monoscale method to both migrated seismic sections and well-log data, we create an image of the earth's local singularity structure. This singularity map facilitates interpretation, facies characterization, and integration of well and seismic data on the level of local texture.

INTRODUCTION

Seismic reflections contain information on regions where the earth's properties vary significantly on the length scale of seismic waves. Mathematically, these regions are represented by zero or first-order transitions, which are singular in their first or second derivatives. Multifractal analysis on well and seismic data (Muller *et al.*, 1992; Saucier and Muller, 1993; Saucier *et al.*, 1997; Herrmann, 1998) demonstrated that variations in the sedimentary upper crust consist of intertwined fractal sets of singularities with different orders. This observation implies three things: First, the global singularity structure of the earth is inherited by the seismic wavefield (Herrmann, 1998), albeit in a bandwidth-limited fashion. Second, traditional transition models are too restricted and need to be generalized to models where the order of the singularities varies fractionally. Third, the multifractality suggests an accumulation of the singularities.

The usefulness of the multifractal framework to upper crust seismic imaging is limited because information on the local characteristics of the singularity structure is lost. This loss withstands a sedimentary facies characterization based on local scaling. Recent results by Alexandrescu *et al.* (1995) and Mallat (1997) show that local Hölder exponents can be estimated from localized decay/growth rate of the wavelet coefficients, along the wavelet transform modulus maxima lines. These Hölder exponents, also known as scale exponents, estimate the *order of magnitudes* of the scaling in the *variations* from both well properties and reflection amplitudes.

Because seismic waves are bandwidth-limited the "multifractal" earth is effectively observed at the scale of one wavelet only. Both the bandwidth limitation and accumulation (the latter gives rise to a mutual interference of the singularities) withstand a successful application of the multiscale wavelet transform to estimate the exponents locally. To tackle these issues a method is proposed which estimates coarse grained, local scale exponents at the fixed scale of the seismic wavelet. The method is based on the property that the β^{th} derivative of a degree α differentiable function diverges when $\beta > \alpha$ (Zähle, 1995). This property translates to the emergence of local maxima for the modulus of a finite resolution observation at the location of the order α transitions. Similar attempts to estimate the scale exponents locally and at a fixed scale have been made using the instantaneous phase (Dessing, 1997; Payton, 1977).

Besides strict locality, additional advantages of the method are the geological interpretation of the exponents, their scale-invariance, their insensitivity to the seismic wavelet and reconstruction capability. More importantly, the sharpness characterization provides a quantitative seismic stratigraphical description of the reflected waveforms which carries information on the depositional and diagenetic environments. Classical seismic stratigraphical models (Payton, 1977) are limited to and composed of aggregates of multiple subwavelength zero- and/or first-order transitions. Characterization by fractional order transitions simplifies these approaches by allowing for a more elaborate sharpness characterization, thus eliminating the necessity to explain the observed waveforms via a superposition of multiple reflectors.

In this paper, we give an overview of the applied techniques by introducing (1) a generalized transition model, (2) a method to analyze the transition's sharpness from both well and seismic data, (3) a method to reconstruct pseudo well-logs from both the location and sharpness of the transitions. Then, we discuss the relevance of the sharpness characterization with respect to seismic facies characterization. Finally, we apply the proposed method to well and seismic data with emphasis on integration of well and seismic data, reconstruction, and depositional facies characterization.

BASIC CONCEPTS AND METHODOLOGY

Seismic waves pick up localized information on regions where the earth's interior varies rapidly on the scale of the seismic wavelet. At those regions, the waves are reflected and mode converted (Herrmann, 2000; Herrmann *et al.*, 2000). Either zero-order jump discontinuities or first-order ramp functions are used to represent these regions. Multi-scale analysis by the wavelet transform, applied to well- and seismic data (Herrmann, 1998), has demonstrated that these transitions are too restricted to represent the wide variety of transitions found in well data. Fractional order transitions are introduced to generalize the representation for the major reflectors. The order of the transitions characterizes the sharpness in a scale invariant manner and depends on the variations in the amplitudes only.

A monoscale analysis is introduced to measure the sharpness directly from well-log data or indirectly from the seismic data. Using the sharpness characterization, maps of the singularity structure of the upper crust are created which are subsequently used for the interpretation and creation of "blocked" (pseudo) well profiles.

Generalized Transitions

Media profiles with transitions of varying order are defined by

$$f(z) = \sum_{i=1}^{N} c_{\pm}^{i} \chi_{\pm_i}^{\alpha_i}(z - z_i) + P_n(z), \tag{1}$$

where the index i runs over the number of transitions, $\pm_i$, $c_{\pm}^{i}$, α_i and z_i determine the direction (positive/negative and causal/anti-causal), magnitude, sharpness and depth location of the transition, respectively (Dessing, 1997; Holschneider, 1995; Herrmann, 1997). The $P_n(x)$ is an n^{th} order polynomial representing the background and

$$\chi_{+}^{\alpha}(z) \triangleq \begin{cases} 0 & z \leq 0 \\ \frac{+z^{\alpha}}{\Gamma(\alpha+1)} & z > 0, \end{cases} \tag{2}$$

$$\chi_{-}^{\alpha}(z) \triangleq \begin{cases} \frac{-z^{\alpha}}{\Gamma(\alpha+1)} & z \leq 0 \\ 0 & z > 0, \end{cases} \tag{3}$$

are the order α onset functions . Only cases where $c_+ \neq 0 \wedge c_- = 0$ or $c_+ = 0 \wedge c_- \neq 0$ are considered. The degree α rules the *sharpness* (regularity) of the transitions which is linked to a local scale-invariance of the type (Herrmann, 1998)

$$\sigma^{-\alpha}\chi_+^\alpha(\sigma z) = \chi_+^\alpha(z) \quad \sigma > 0. \tag{4}$$

For $\alpha = 0$, $f(z)$ has a jump discontinuity for which the renormalization is scale independent; for $\alpha = 1$, the onset function is a ramp function, for which the renormalization is the reciprocal of the scale. Irrespective of any particular scale the exponent α quantifies the sharpness and the *order of magnitude* of the variations in the data. Figure 1 illustrates both the sharpness and directionality of fractional order transitions and their relation with the signature/waveform of the reflection events. Figure 2 (top) contains an example of a medium profile with five different onset functions.

Monoscale Sharpness Analysis

Multiscale wavelet transforms are normally used to characterize the order of transitions/edges (Herrmann, 1998; Herrmann and Stark, 1999). Focusing on these orders has the advantage of being less prone to measurement, model and calibration errors as compared to analyzing the reflection amplitudes only. Unfortunately, multiscale methods are not applicable when the scale/bandwidth content of the data is too limited or when the data contain too many interfering transitions. Both situations apply to well and seismic data, withstanding a successful estimation of the local scale exponents.

By extending the ordinary wavelet transform,

$$\mathcal{W}\{f,\psi^M\}(\sigma,z) \triangleq \sigma^M \frac{\mathrm{d}^M}{\mathrm{d}z^M}(f * \phi_\sigma)(z), \tag{5}$$

for varying scale, σ, and fixed number of vanishing moments, M, to a transform with the scale fixed and wavelet order, β, varied fractionally (Herrmann, 2000; Stark and Herrmann, 2000),

$$\mathcal{W}\{f,\psi^\beta\}(\sigma,z) \triangleq \overbrace{\sigma^\beta \frac{\mathrm{d}^\beta}{\mathrm{d}z^\beta}}^{\text{(de-) sharpening}} \underbrace{(f * \phi_\sigma)(z)}_{\text{smoothing}} \quad \text{for} \quad \beta \in \mathbb{R} \quad \text{and} \quad \sigma > 0, \tag{6}$$

different types of transitions from both broadband well and single band seismic data can be analyzed. The dependent variable z refers to either the time or space coordinate. For integer[1] values ($\beta = M$) the function ϕ_σ is a sufficiently smooth ($2M$ differentiable) smoothing function with support σ, and ψ_σ^M in a wavelet generated by dilations of $\psi^M(z) = (-1)^M \frac{\mathrm{d}^M}{\mathrm{d}x^M}\phi(z)$.

For $\beta = 0$ the convolution with ϕ, chosen to be a Gaussian bell shape function with a width proportional to the scale σ, represents a smoothing of the well-log. For $\beta = 1$

[1] Generally these statements translate to the fractional case.

Eq. 6 corresponds to the depth-traveltime converted reflectivity based on a convolution model (Herrmann, 2000),

$$p(z,t) \approx \frac{\mathrm{d}}{\mathrm{d}t}(\zeta * \varphi_{\text{seis}})(t) = {\sigma_{\text{seis}}}^{-1}\mathcal{W}\{\zeta, \varphi_{\text{seis}}\}(\sigma_{\text{seis}}, t), \tag{7}$$

where φ_{seis} is the seismic wavelet with a scale, σ_{seis}, and $\zeta(t)$ the time parameterized log acoustic impedance or impedance fluctuation. Eq. 7 has the form of an ordinary wavelet transform (cf. Eq. 6 for $\beta = 1$) with the scale set to the fixed seismic scale.

By controlling the sharpening $\beta > 0$ for the well analysis or the de-sharpening $\beta < 0$ for the seismic data, the location and order of the transitions can be found via the following two on-off criteria (Herrmann, 2000; Herrmann *et al.*, 2000; Stark and Herrmann, 2000):

- For transitions with $\alpha \geq 0$ and $\beta \in \mathbb{R}^+$,

$$\alpha(\sigma, z) = \inf_{\beta}\{\partial_z \mathcal{W}_\beta\{f, \phi\}(\sigma, z) = 0\}. \tag{8}$$

- For reflection events with $\alpha < 0$ and $\beta \in \mathbb{R}_0^-$,

$$\alpha(\sigma, z) = \sup_{\beta}\{\partial_z \mathcal{W}_\beta\{f, \phi\}(\sigma, z) = 0\}. \tag{9}$$

For a positive order onset function ($\alpha \geq 0$) a local modulus maximum emerges when the order of fractional differentiation ($\beta > 0$) in Eq. 6, infinitesimally exceeds the order of the transition α. Conversely, for a differentiated transition, i.e. a reflection event with $\alpha < 0$, the local modulus maxima disappear when the order of fractional integration ($\beta \leq 0$) infinitesimally exceeds the negative order α. Exponents estimated at a particular finite scale by these criteria are referred to as coarse grained Hölder exponents, which as the scale goes to zero, converge to the true Hölder exponents (Zähle, 1995).

Figures 1 and 2 show that the onset functions can be causal/anti-causal and/or flipped in sign. The onset-criteria of Eqs. 8 and 9 are affected by this directivity. To circumvent this problem, the monoscale analysis (cf. Eqs. 6-9) is conducted using both causal and anti-causal fractional derivatives or integrals. Figure 2 contains an example with smoothed causal and anti-causal onset functions submitted to the analysis. The location and direction of the singularities (third plot) are correctly estimated.

Reconstruction

Most information on the variability in well and seismic data is contained in the location and order of the singularities. Monoscale analysis provides this information which, when supplemented with information on the reflection amplitudes at the location of the singularities, can be used to construct "blocked" pseudo well profiles, with varying order transitions (cf. Eq. 1 without the $P_n(z)$). The term pseudo refers to reconstruction

modulo polynomials, i.e., the smooth/trend is not reconstructed. The bottom plot of Figure 2 contains the reconstruction of the synthetic example depicted on the top. Estimates for the location, order, direction and relative magnitude are taken from both the second and third plot. The smoothing of the original function is removed by setting the smoothing of the reconstruction to zero. Deviations in the reconstruction in between the transitions (e.g., between the first and the second) are due to the fact that the method is only sensitive to singular variations.

APPLICATION TO WELL DATA

In Figures 3 and 4 the monoscale method is applied to an acoustic impedance profile obtained from a well-log measurement (depicted on the left). The log is (from left to right) increasingly smoothed. The position of the balls points to de positions of the singularities. The color refers the order while the size of the balls contains information on the magnitude of the smoothed derivative *at* the location of the singularity. The fact that well-data behave multifractally (see, e.g., Herrmann, 1997) is evident from the irregular color changes of the balls. In addition the emergence of the balls almost everywhere is an indication of an accumulation of the singularities, a result also consistent with the multifractal findings.

Figure 4 contains a pseudo well (middle) and reflectivity (bottom) obtained from the coarse scale attribute analysis applied to the impedance log on the top (cf. Figure 3). Although the reconstruction is not perfect, the result is encouraging because the pseudo reflectivity matches the reflectivity from the original well. Clearly the proposed reconstruction scheme corresponds in this context to a ***generalized blocking***, including fractional transitions.

APPLICATION TO SEISMIC DATA

The results of the monoscale method, applied to a selection of three traces of the Mobil post-stack migrated data set, are depicted in Figure 6. In this plot the location, color and size of the balls refer to the location of the reflector, its order and relative magnitude. Clearly, there are different order singularities present in the reflection data. Figure 5 contains a comparison of the original *versus* pseudo reflectivity, generated from a trace of the time migrated Gulf of Mexico data set (top) together with its tie (bottom). Finally, Figures 7–9 show an example of the application of the method to a section of a time-migrated Mobil data set. The position and order of the reflections are depicted by the location and color of the dots (see Figure 8). The corresponding orders for the reflectors, the transitions causing the reflections, can readily be obtained when the order of the seismic wavelet is known, e.g., for a Ricker wavelet one simply adds 3. The results of Figure 8 demonstrate that the proposed method captures the location and sharpness of the reflectors in a consistent manner unaffected by lateral variations in amplitude. The migrated section in Figure 7 can be reconstructed, using the scale attributes depicted

in the Figure 8. The pseudo reflectivity is plotted in Figure 9 and shows a beautiful agreement with the section in Figure 7.

WELL TIE

Figures 10 through 12 illustrate an example where well and seismic data are tied on the level of the attribute. First a wavelet is estimated, minimizing the mismatch between the migrated seismic data and modeled acoustic normal incidence reflectivity. An acoustic layercode program is used to calculate the reflectivity from the well. Figure 10 displays the migrated and modeled traces in the top two plots. The wavelet, establishing the tie is estimated by generating a family of wavelets, defined by shifts, dilations and fractional differentiations of a Gaussian bell-shape function. The optimal order for the wavelet is found to be $\alpha_{wav} = 1.22$, which is slightly more than the first derivative. The estimated wavelet in displayed on the bottom row of Figure 10 and closely resembles the wavelet measured from the airgun see (Keys and Foster, 1998).

Comparisons between the modeled and migrated data can be found in the third row of Figure 10 and in Figure 11. The obtained fit is not perfect. Events are missing in the synthetic (around $t = 1.8\,\mathrm{s}$) as well as in the migrated data (below $t = 2.2\,\mathrm{s}$).

The section with the tie, the middle traces from #25 to #30, is depicted in Figure 11. This section serves as input for the attribute analysis, which is on display in Figure 12. The meaning of the color balls is the same as in the previous examples. One can see that on the level of the attribute there is a good correspondence between the seismic section and the well synthetic. Not only the lateral consistency is good for many reflector horizons but also the estimated attribute values integrate nicely across the seismic and synthetic. At this point issues related to seismic stratigraphy may be addressed.

FACIES CATEGORIZATION BY SHARPNESS CHARACTERIZATION

The permeability and porosity distribution of sedimentary rock is dependent mainly on the depositional and diagenetic environments of the sediments. The depositional environment refers to the energy level of the depositional system, which is mainly responsible for the sorting of the particles. The Jurassic reservoirs in the analyzed North Sea[2] data set range in depositional environment from fluvial to deltaic and shallow marine (Keys and Foster, 1998).

In line of Harms and Tackenberg (1972), a suite of three simplified models for the lithologic boundaries is proposed. The nature of these boundaries is related to the sorting of the sands. When assuming the compressional wavespeed to increase with sand content the sorting is directly related to the characteristics of the velocity profile. The three facies types under consideration are

[2]Courtesy of Mobil, who provided a data set for evaluating and comparing seismic inversion methods (Keys and Foster, 1998).

- **shallow marine/nearshore**: where the upper contact tends to be sharp, see Figure 13 (top).
- **channel**: where the lower contact is sharp, see Figure 13 (middle).
- **turbidity**: where both the top and bottom are marked by sharp onsets, see Figure 13 (bottom).

For the nearshore facies the sandstone is cleanest at the top where the coarsest sands are deposited. The base is transitional with the underlying mudrock. Consequently, the velocities will be highest at the top and then go down as the sand becomes dirty. For channels an opposite behavior is observed. In that case the largest velocities are found at the bottom where the coarsest, hence cleanest, sands reside. Finally, a symmetric profile is introduced to model the behavior of a turbidity sandstone.

Onset functions defined in equations 2 and 3 provide the perfect vehicle to model these three types of transition zones. By setting the sharpness to a negative value, $-1 < \alpha < 0$ asymmetric profiles can be generated of varying sharpness and with exactly similar characteristics as the shallow marine/nearshore and channel facies. In this example the value for α was set to $\alpha = -0.75$. To give the transitions spatial extend the transitions are smoothed with a Gaussian bell-shape function. Finally, the turbidity phase is defined as a symmetric cusp with the same scale exponent.

All three examples in Figure 13 display the same scaling behavior. The directivity, however is different a notion recovered by the monoscale analysis presented in this paper. In a future paper more attention will be paid to this issue. Besides the directivity the sharpness α may vary indicating differences in the sorting. The smaller the α the steeper the profile becomes.

CONCLUSIONS

A powerful new tool has been developed which allows for the introduction of a new attribute. This attribute characterizes the sharpness of the reflectors and allows for the construction of pseudo wells and seismic data. Both the location and the value of the attribute are estimated in a laterally consistent way, revealing a structural image. Because sharpness describes the local texture a possibility is created to infer information on the depositional environment underlying the stratigraphy.

ACKNOWLEDGMENTS

This work was supported by the Borehole Acoustics and Logging/Reservoir Delineation Consortia at the Massachusetts Institute of Technology.

REFERENCES

Alexandrescu, M., D. Gilbert, G. Hulot, J.-L. Le Mouël, and G. Saracco, Detection of geomagnetic jerks using wavelet analysis, *J. Geophys. Res.*, *100*, 12,557–12,572, 1995.

Dessing, F.J., A wavelet transform approach to seismic processing, Ph.D. thesis, Delft University of Technology, Delft, The Netherlands, 1997, `http://wwwak.tn.tudelft.nl/~frankd`.

Harms, J.C. and P. Tackenberg, Seismic signatures of sedimentation models, *Geophysics, 37,* 45–58.

Herrmann, F., A scaling medium representation, a discussion on well-logs, fractals and waves, Ph.D. thesis, Delft University of Technology, Delft, The Netherlands, 1997, `http://wwwak.tn.tudelft.nl/~felix`.

Herrmann, F., Multiscale analysis of well and seismic data, in S. Hassanzadeh (ed.), *Mathematical Methods in Geophysical Imaging V*, vol. 3453, pp. 180–208, SPIE, 1998.

Herrmann, F., A scale attribute for texture in well- and seismic data, *Geophys. J. Internat.*, in preparation, 2000.

Herrmann, F., and C. Stark, Monoscale analysis of edges/reflectors using fractional differentiations/integrations, in *Expanded Abstracts, Soc. Expl. Geophys.*, Tulsa, 1999, `http://www-erl.mit.edu/~felix/Preprint/SEG99.ps.gz`.

Herrmann, F., S. Chevrot, and C. Stark, Sharpness characterization of upper mantle discontinuities by fixed scale singularity analysis of converted phases, *Geophys. J. Internat.*, in preparation, 2000.

Holschneider, M., *Wavelets: An Analysis Tool*, Oxford Science Pub., 1995.

Keys, R., and D. Foster, *Comparison of Seismic Inversion Methods on a Single Real Data Set*, Soc. Expl. Geophysicists, 1998.

Mallat, S.G., *A Wavelet Tour of Signal Processing*, Academic Press, 1997.

Muller, J., I. Bokn, and J.L. McCauley, Multifractal analysis of petrophysical data, *Ann. Geophysicae*, *10*, 735–761, 1992.

Payton, C. (editor), Stratigraphic model from seismic data, in *Seismic Stratigraphy—Applications to Hydrocarbon Exploration,* AAPG, 1977.

Saucier, A., and J. Muller, Use of multifractal analysis in the characterization of geological formation, *Fractals*, *1*, 617–628, 1993.

Saucier, A., O. Huseby, and J. Muller, Multifractal analysis of dipmeter well logs for description of geological lithofacies, in *Fractals in Engineering*, Springer, 1997.

Stark, C., and F. Herrmann, Monoscale wavelet analysis and its application to streamflow time series, *Geophys. Res. Lett.*, to be submitted, 2000.

Zähle, M., Fractional differentiation in the Self-Affine case: V-The local degree of differentiability, *Math. Nachr.*, 1995.

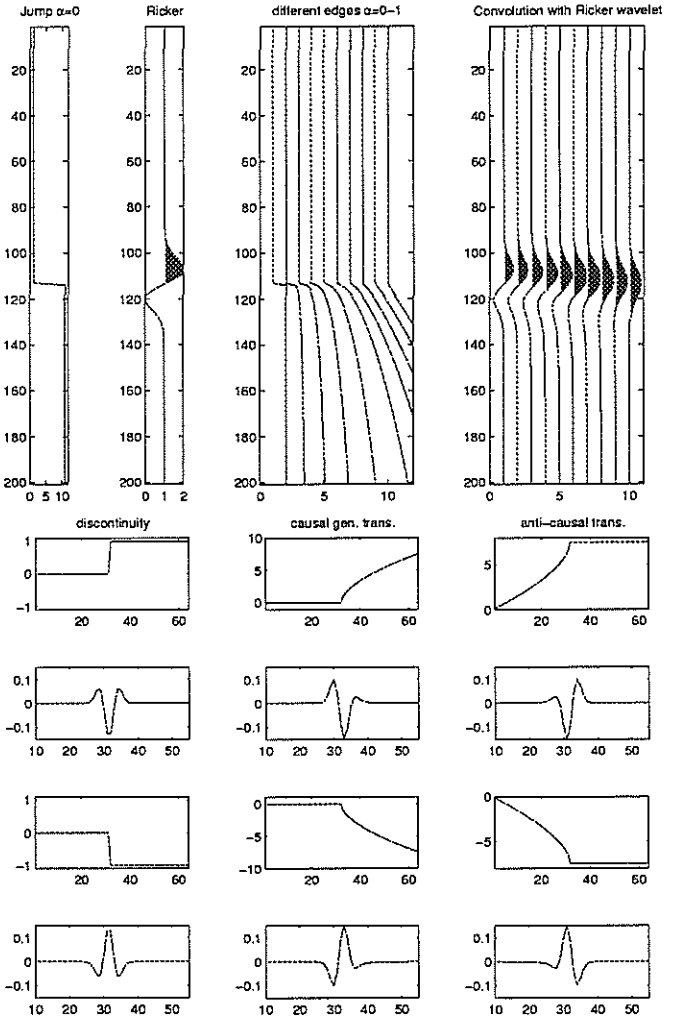

Figure 1: Generalization of edges from a jump on the top left to fractional edges with $\alpha \in (0, 1)$ on the top right. The signature of the normal incident amplitude normalized reflections (Ricker wavelet) clearly depend on the order. The direction of the onsets also plays a role as seen in the second half of this figure.

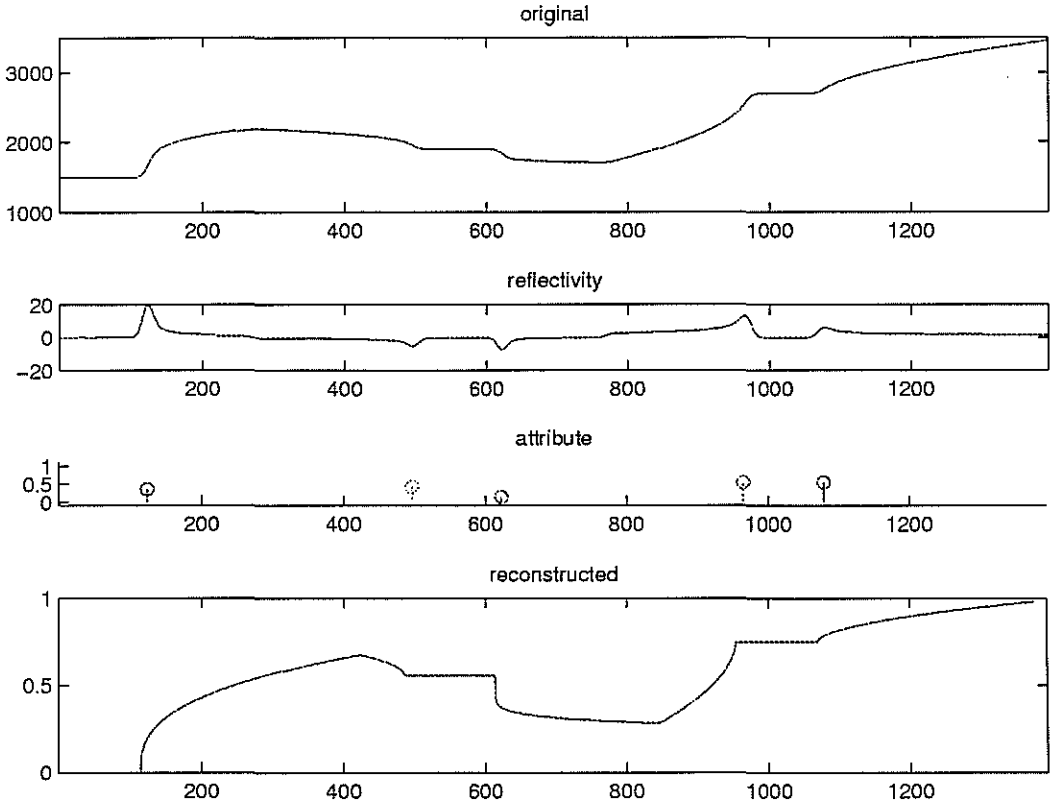

Figure 2: Example of analysis and reconstruction of a synthetic well with different order singularities and directions. (top) the synthetic well with 5 smoothed singularities; (second plot) "reflectivity"; (third plot) position, order and direction singularities. Blue is causal positive, green anti-causal positive, red causal negative sign, magenta anti-causal negative sign. (bottom) the reconstructed profile.

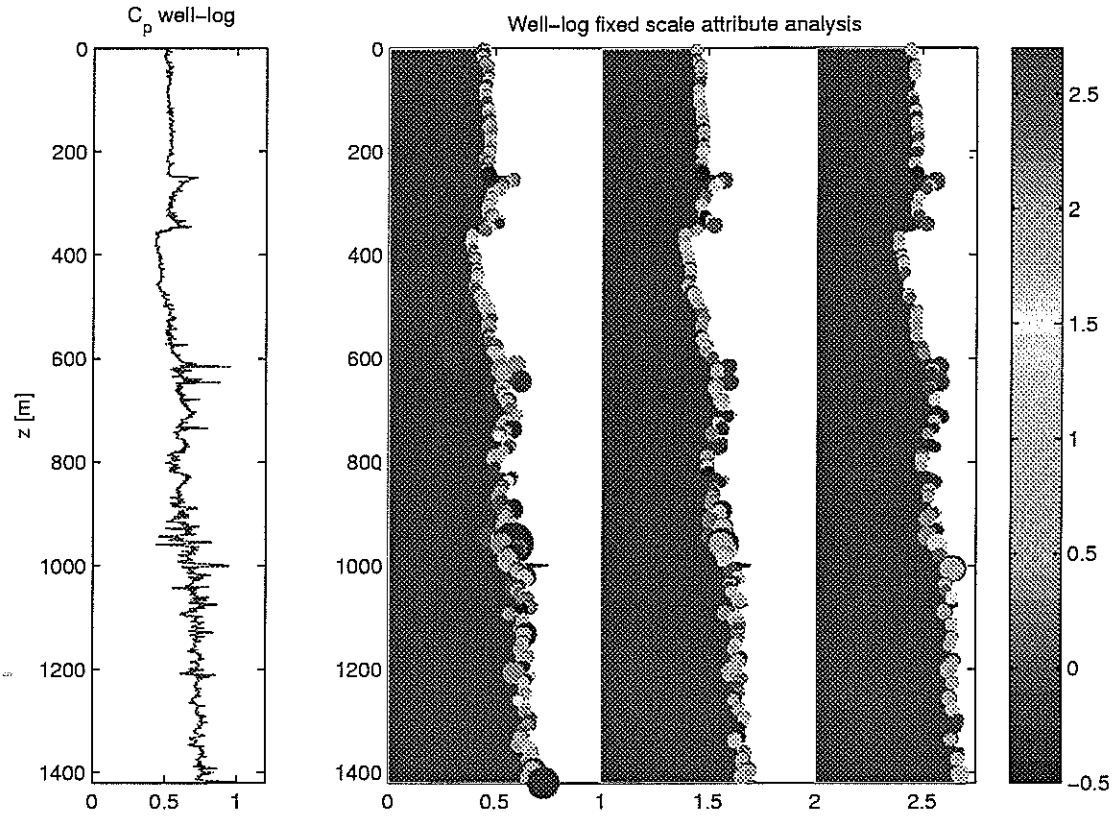

Figure 3: Application of monoscale method to Mobil well-data (Keys and Foster, 1998).The color coding refers to the values for the estimates of the local scale exponent. The sizes of the balls are related to the magnitude of the wavelet coefficients (the derivative/"reflectivity") at the location of the singularity. The different traces refer to different smoothings of the well on the left. The heterogeneity of the scaling becomes clear from the changing in color of the attribute α plotted on top of the logs. The color bar shows the corresponding values for the estimates. Finally, notice that the volatility in the ball sizes becomes smaller for the larger scales.

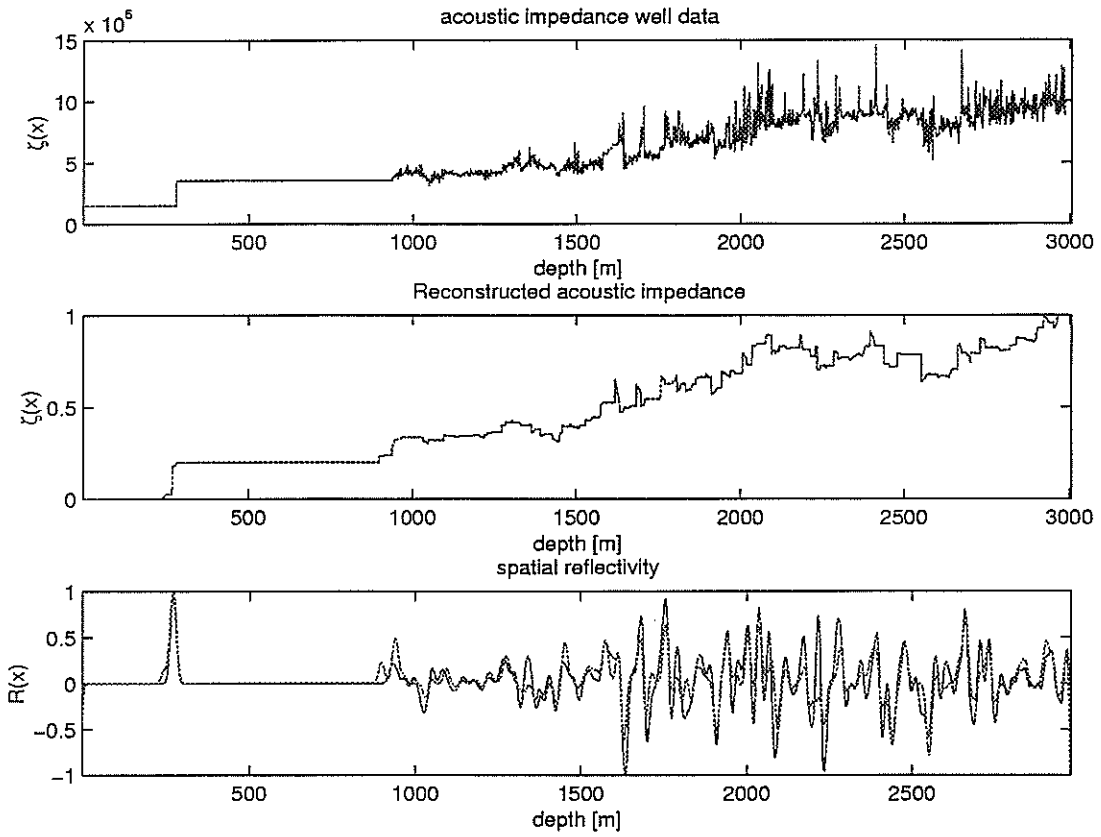

Figure 4: Application of monoscale method to Mobil well-data set. (top) acoustic impedances; (middle) reconstructed pseudo well, based on the scale attribute and estimated at the scale of the reflectivity (bottom). The pseudo well contains different order transitions and yields a pseudo reflectivity that is close to the one of the well on the top.

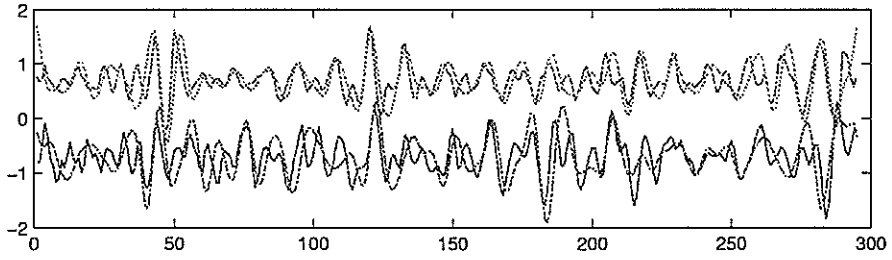

Figure 5: Pseudo *versus* original time migrated traces from the Gulf of Mexico, tied with a synthetic. On the top comparison for the synthetic on the bottom for the migrated data (courtesy Schlumberger).

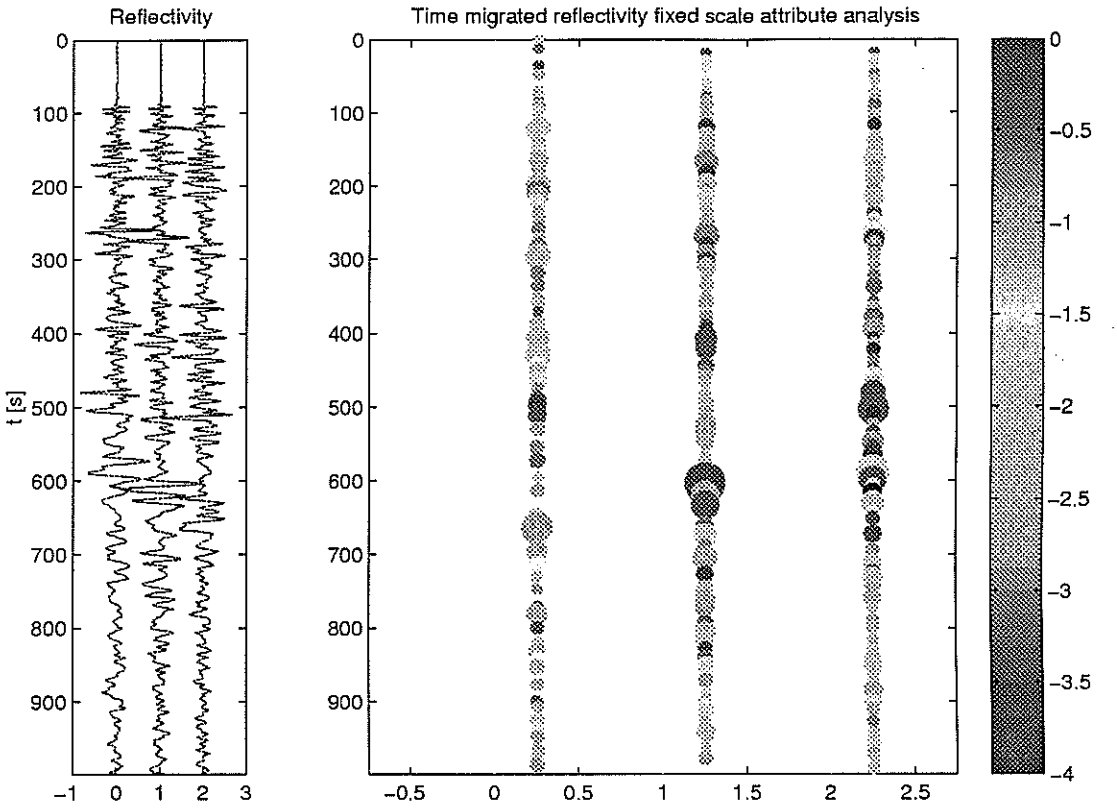

Figure 6: Application of the monoscale method to 3 traces of the Mobil time migrate data (see Fig. 7). The color of balls refers to the order and the size to the reflection magnitude. The estimated exponents are mostly negative because reflection entails differentiation.

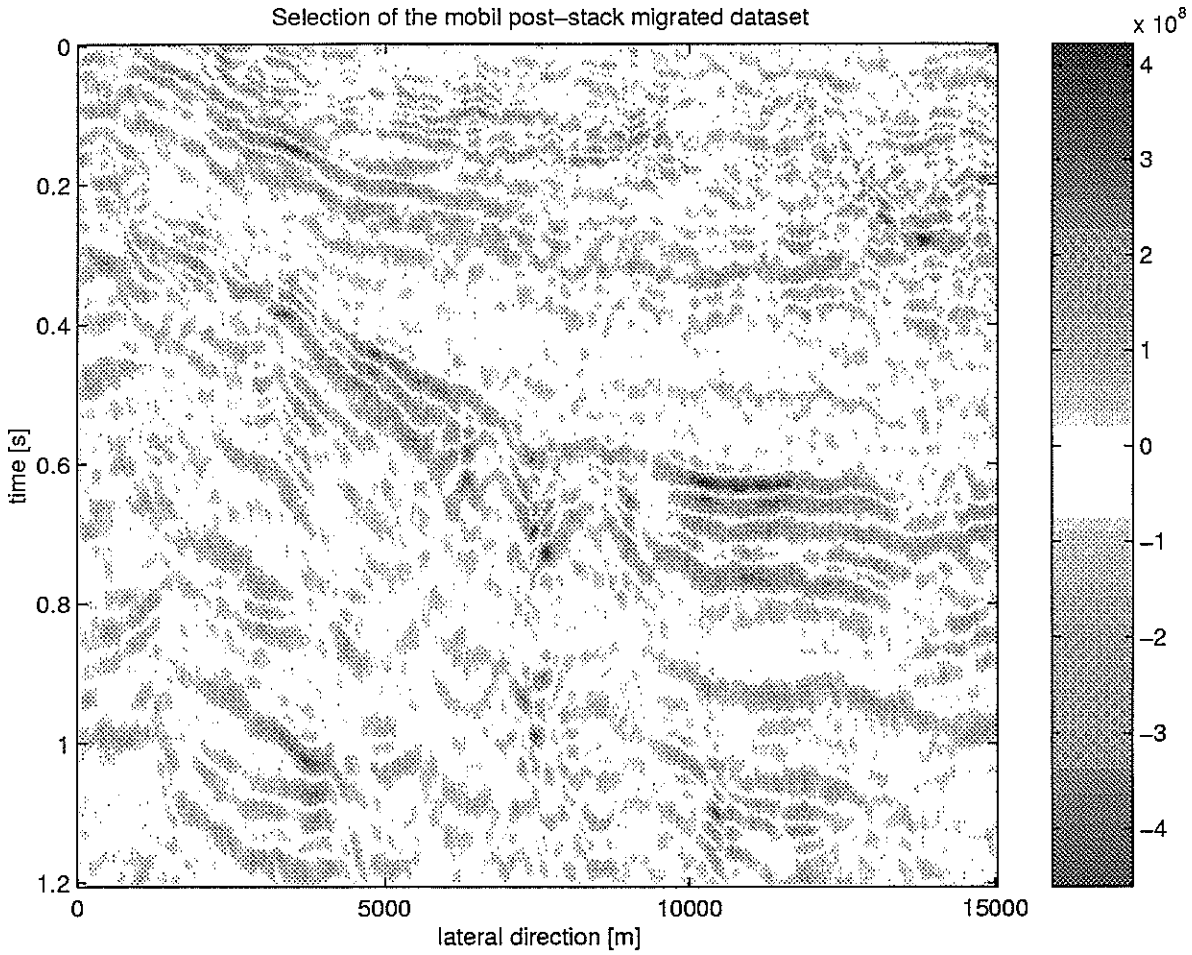

Figure 7: Time migrated section from the Mobil data set.

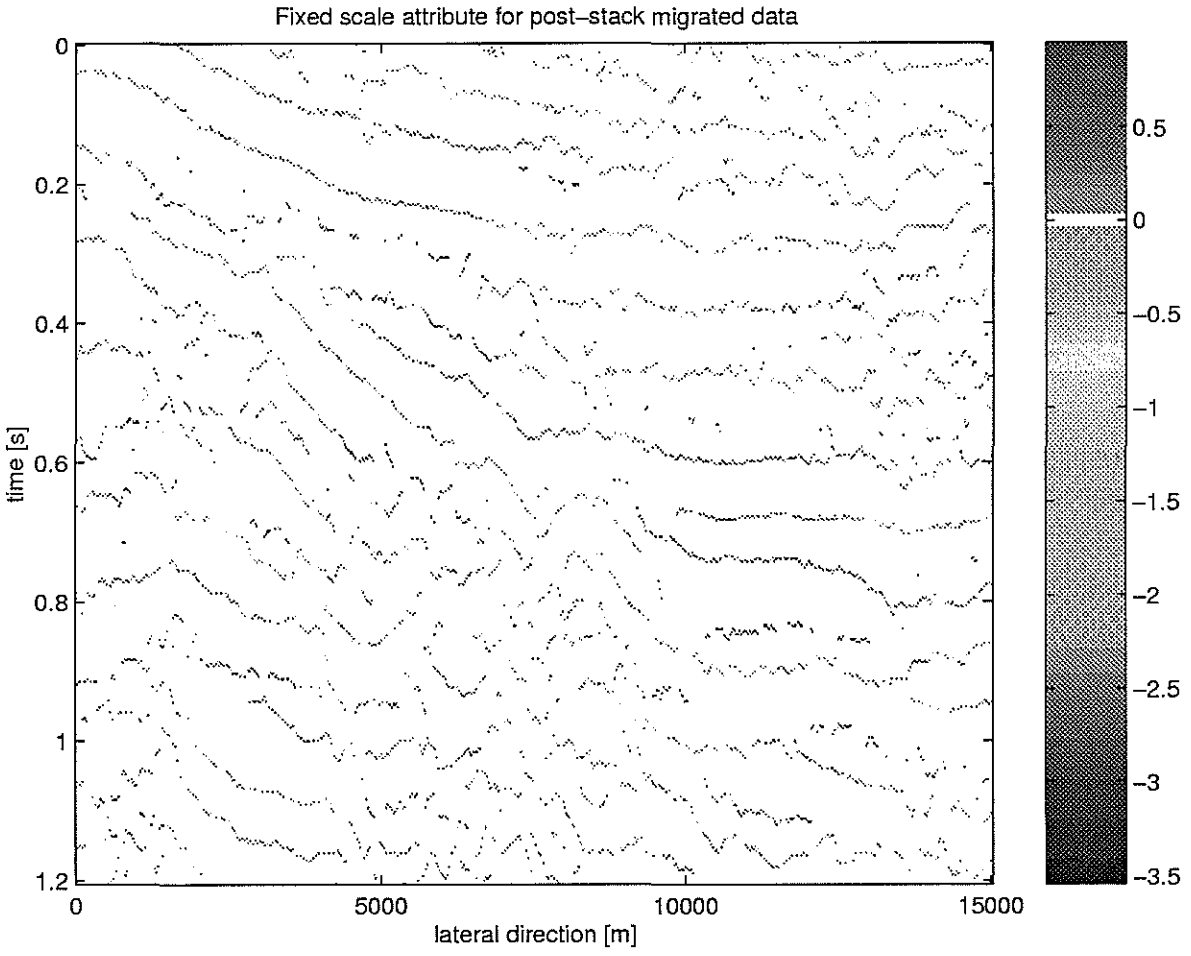

Figure 8: Attribute.

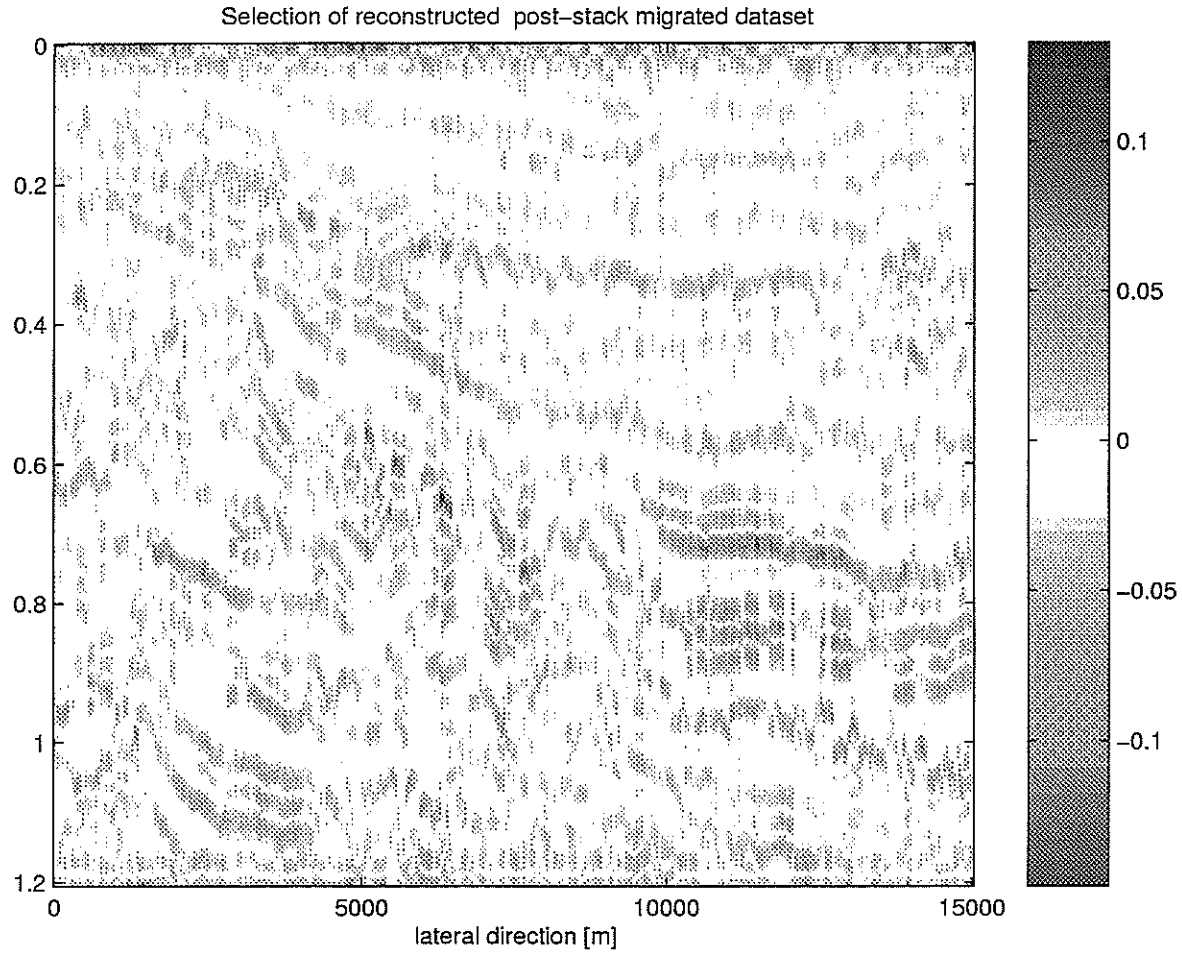

Figure 9: Reconstruction.

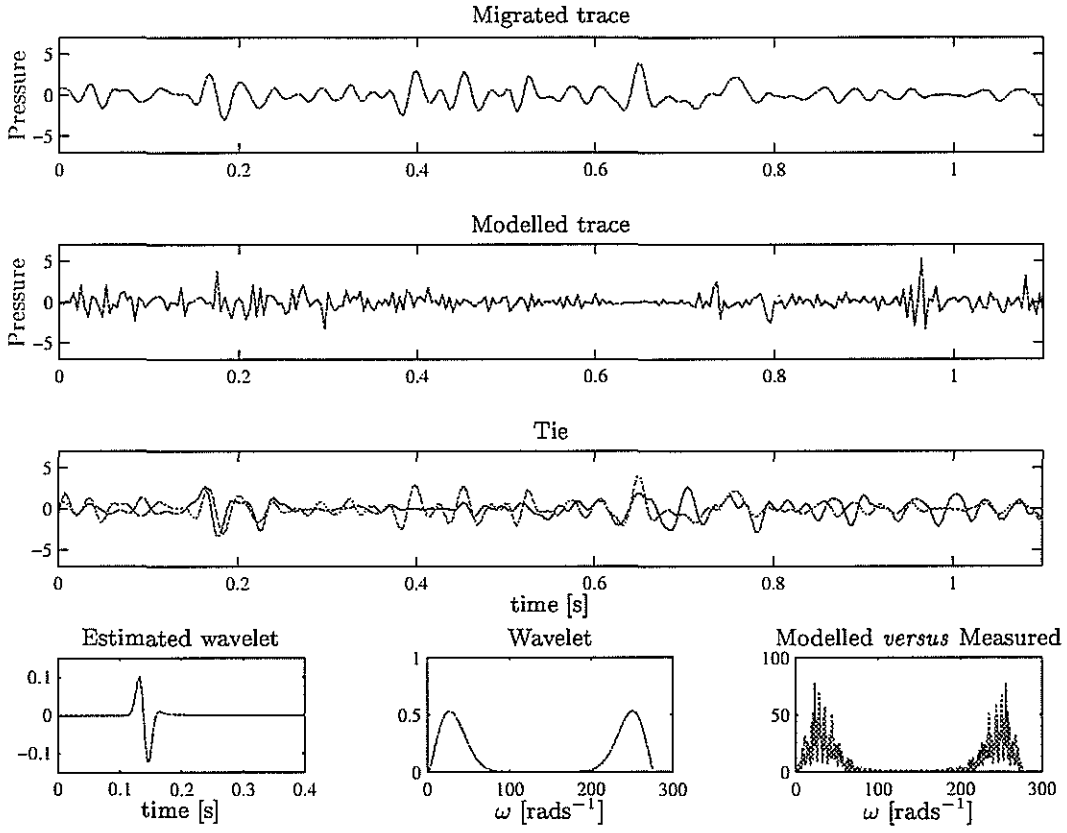

Figure 10: Wavelet estimation by minimizing the difference between the imaged seismic reflectivity (top) and the modeled reflectivity (second plot). The optimal tie is depicted in the third plot. On the bottom row the estimated wavelet and frequency spectrum are displayed together with the spectrum of the tie. The wavelet provides a reasonable tie and is close to the wavelet estimated from the airgun (see Keys and Foster, 1998).

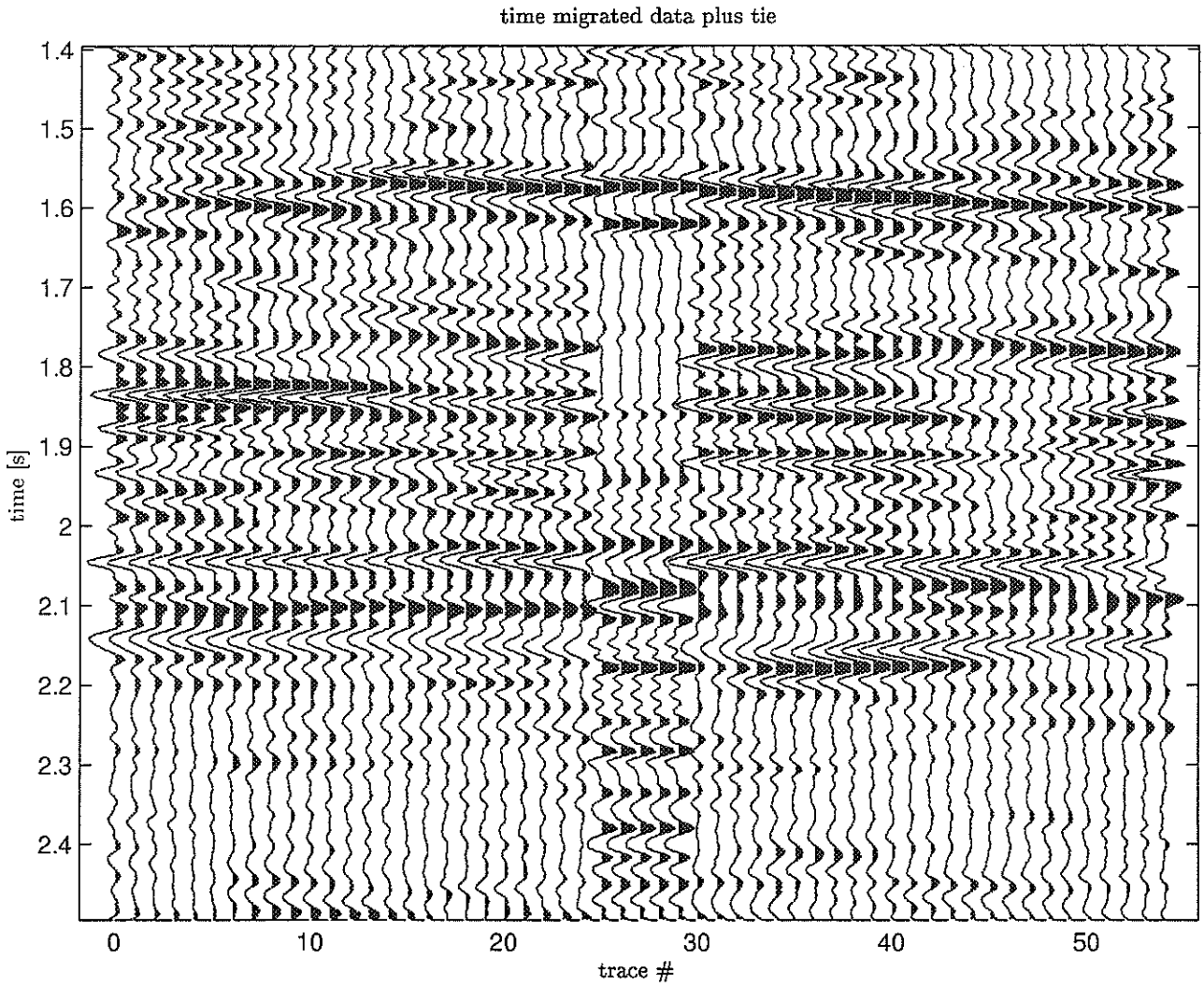

Figure 11: Migrated section and the tie in the middle. The major reflection events are captured reasonably well. Still in the modelled data there are events missing around $t = 1.8\,\mathrm{s}$. Below $t = 2.2.\,\mathrm{s}$ the seismic data does not show significant activity.

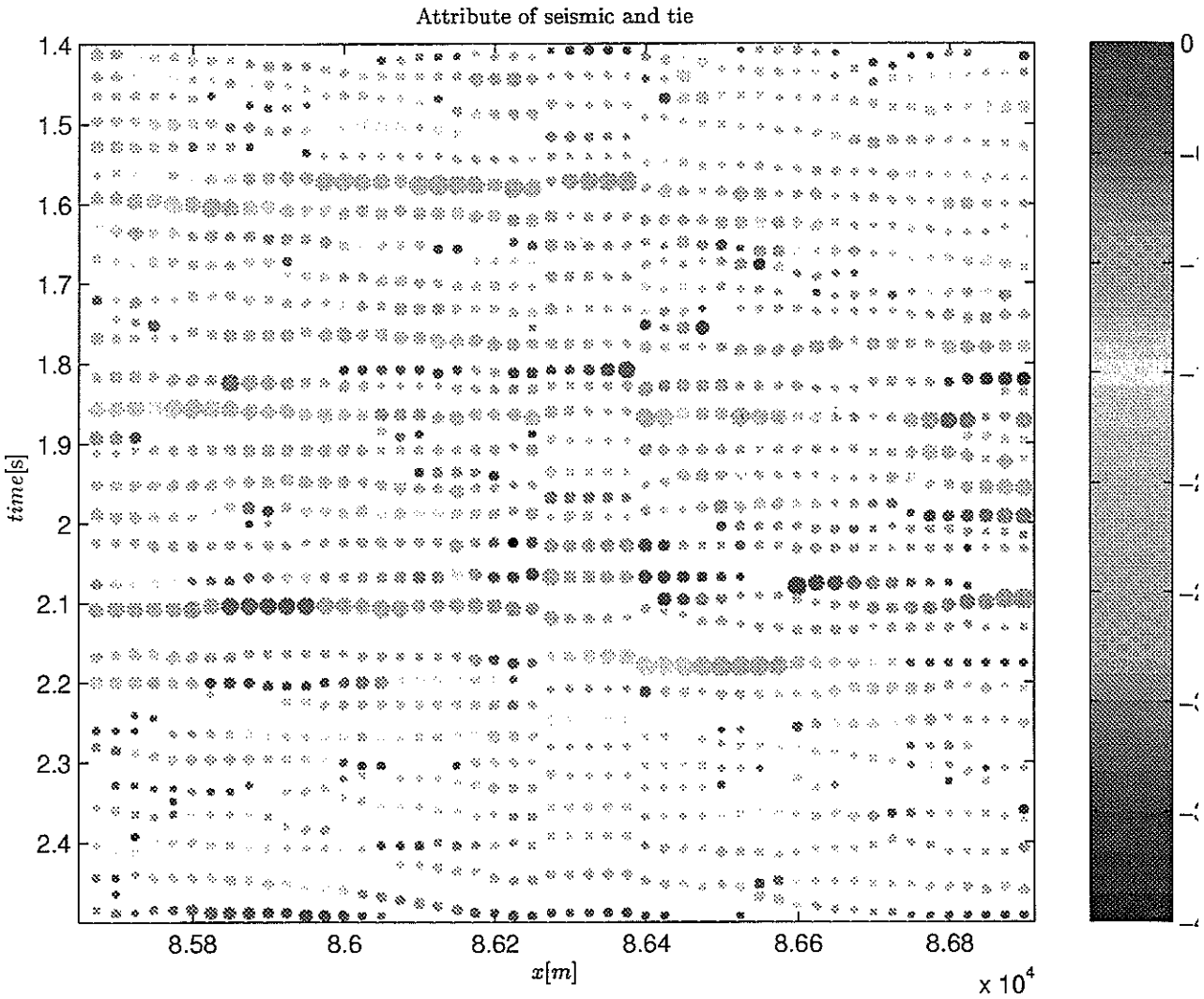

Figure 12: Attribute analysis of the section depicted in Figure 11. Notice the good agreement between the seismic section and the synthetic.

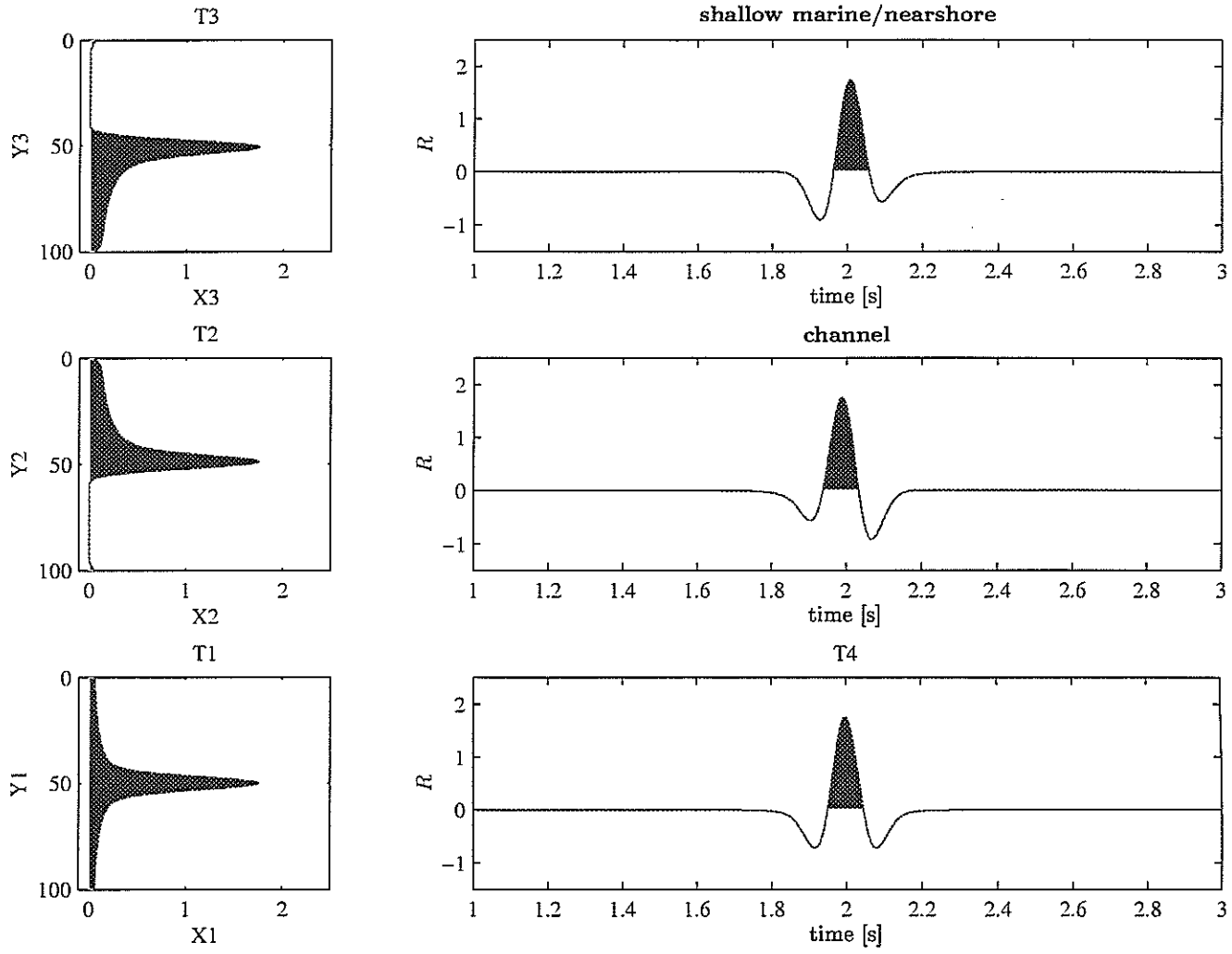

Figure 13: Example of application of the generalized transition concept to a possible facies identification. Three different facies are introduced, representing shallow marine/nearshore, channel and turbidity depositional environments. These environments are modeled by a causal, anti-causal and symmetric onset functions as defined by equations 2 and 3 with α set to $\alpha = -0.75$. In order to create a spatial extend the onset functions are convolved with a Gaussian bell-shape function. In the left column the velocity profiles are depicted. On the right the corresponding reflection responses. Notice that these transitions all scale the same.